

RESEARCH

Open Access



# Polydopamine-based nano-protectant for prolonged boar semen preservation by eliminating ROS and regulating protein phosphorylation via D2DR-mediated cAMP/PKA signaling pathway

Lirui Wang<sup>1</sup>, Manyi Xiong<sup>1</sup>, Jian Zhang<sup>2</sup>, Sisi Li<sup>1</sup>, Sheng Ma<sup>1</sup>, Shengyao Jiang<sup>1</sup>, Yanping Jiang<sup>1</sup> and Xinhong Li<sup>1\*</sup>

## Abstract

**Introduction** Preservation of porcine semen is essential for artificial insemination and genetic improvement in pig breeding programs. However, the overproduction of reactive oxygen species (ROS) and lower levels of protein phosphorylation emerge as two challenges during semen preservation. Inspired by the innate ligand-receptor binding biofunction of dopamine, herein, a dual-task nano-protectant that combines ROS-scavenging and protein phosphorylation-regulating properties via incorporating the natural antioxidant epigallocatechin gallate (EGCG) into polydopamine nanoparticles (EGCG@PDA NPs) was proposed to enhance the quality of pig semen during storage at 4 °C. The results suggested that EGCG@PDA NPs significantly maintained sperm motility, acrosome integrity and mitochondrial membrane potential, extending semen storage time from 3 days to 10 days. Furthermore, EGCG@PDA NPs effectively scavenged excess ROS and inhibited ROS-mediated sperm apoptosis through the extracellular regulated protein kinases (ERK) signaling pathway. Intriguingly, EGCG@PDA NPs could degrade into ultrasmall particles (< 10 nm) in the semen or H<sub>2</sub>O<sub>2</sub> systems. These particles could target and activate the dopamine D2 receptor (D2DR) on membrane surface of sperm midpiece, thereby enhancing protein phosphorylation via the downstream cyclic adenosine monophosphate/protein kinase A (cAMP/PKA) signaling pathway, ultimately improving sperm motility parameters. This study presents a novel nano-strategy to boost the quality of pig semen, offering significant implications for the pig industry.

**Keywords** Semen preservation, Polydopamine nanoparticles, ROS, Protein phosphorylation, D2DR

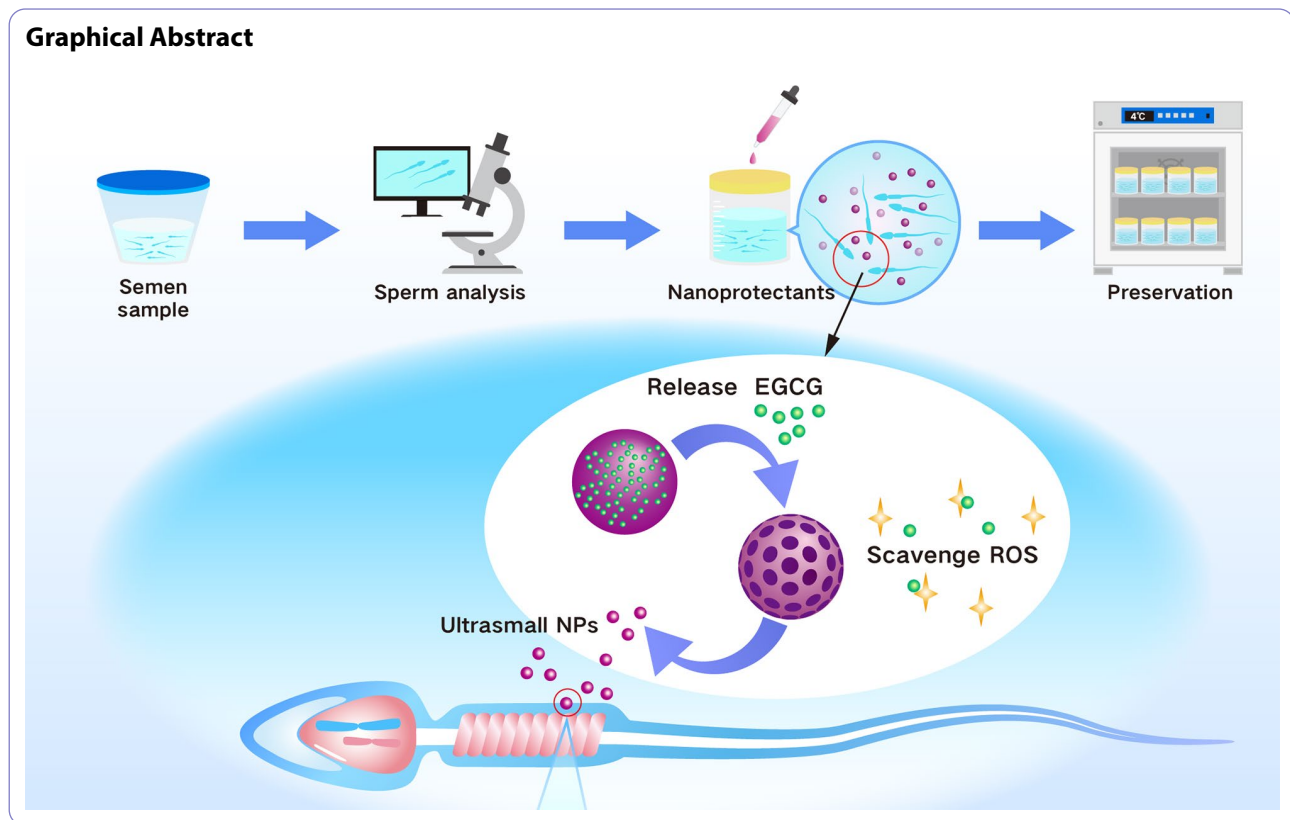
\*Correspondence:

Xinhong Li  
lixinhong7172@sjtu.edu.cn

Full list of author information is available at the end of the article



© The Author(s) 2025. **Open Access** This article is licensed under a Creative Commons Attribution-NonCommercial-NoDerivatives 4.0 International License, which permits any non-commercial use, sharing, distribution and reproduction in any medium or format, as long as you give appropriate credit to the original author(s) and the source, provide a link to the Creative Commons licence, and indicate if you modified the licensed material. You do not have permission under this licence to share adapted material derived from this article or parts of it. The images or other third party material in this article are included in the article's Creative Commons licence, unless indicated otherwise in a credit line to the material. If material is not included in the article's Creative Commons licence and your intended use is not permitted by statutory regulation or exceeds the permitted use, you will need to obtain permission directly from the copyright holder. To view a copy of this licence, visit <http://creativecommons.org/licenses/by-nc-nd/4.0/>.



## Introduction

The demand for premium pig semen of high quality or high genetic value has surged due to the expanding pig industry and the necessity for genetic improvement. Maintaining the viability and fertility of spermatozoa during semen preservation is crucial for artificial insemination. Among various preservation methods, storing porcine semen at 4 °C offers notable advantages over cryopreservation and room temperature storage [1–3]. However, boar spermatozoa are particularly susceptible to low temperatures [4–6], ascribing to their low cholesterol/phospholipid ratio, which predisposes them to oxidative damage from excessive reactive oxygen species (ROS) production. Consequently, pig semen quality can rapidly decline under conventional preservation conditions, leading to reduced fertility rates and substantial economic loss. Another significant issue during boar semen preservation is the reduction in protein phosphorylation levels [7]. Notably, the protein phosphorylation is positively correlated with boar sperm motility [8] and is a crucial mechanism by which cyclic adenosine monophosphate/protein kinase A (cAMP/PKA) signaling pathway regulates sperm motility [9], suggesting that enhancing protein phosphorylation via cAMP/PKA pathway could therefore optimize preservation effects. Thus, addressing these two challenges is the key to improve semen preservation quality.

With advancements in nanotechnology, the application of nanoparticles in the field of reproduction has gradually become a research hotspot, particularly antioxidant nanoparticles such as fullerenes C60 [4] and selenium nanoparticles [10]. However, nanoparticles possessing only single antioxidant property are insufficient for addressing complex practical issues [11]. Furthermore, nanoparticles have been explored for combination therapy in treating various diseases such as cancer [12, 13]. Consequently, developing a dual-functional nanoprotectant that both acts as antioxidant and enhances protein phosphorylation may be an effective way to improve the quality of boar semen preservation.

Polydopamine nanoparticles (PDA NPs), formed by the self-polymerization of dopamine molecules, have received tremendous interest recently ascribing to their excellent biocompatibility and versatility in applications such as drug delivery [14–16], inflammation regulation [17, 18], biosensing [19, 20] and tissue engineering [21, 22]. Recent investigations have revealed the potential antioxidant property of PDA NPs, featured by plentiful phenolic hydroxyl groups serving as potent free radical scavengers, to reduce damage from ROS or acute inflammation [23–25]. Additionally, the inherent ligand-receptor binding capability of dopamine molecule endows PDA NPs with superior biotargeting functionality [26]. Dopamine receptors that belong to G-protein-coupled

receptor family, have been identified in the sperm of several different species, including humans, rats, mice, bulls and boars [27–29]. Previous investigations have shown that when dopamine binds to the dopamine D2 receptor (D2DR) of spermatozoa, it triggers a signaling cascade that influences the activity of protein kinases and phosphatases, leading to the phosphorylation of specific tyrosine residues of proteins, crucial for regulating sperm motility [27, 29]. It is hypothesized that the activation of D2DR may be a vital target for modulating protein phosphorylation and thus regulates sperm viability via the downstream cAMP/PKA pathway.

EGCG, the major catechin in green tea, is known for its anti-inflammatory, antioxidant, and anti-cancer properties and has been extensively studied for its potential health benefits. Additionally, supplementation of spermatozoa with EGCG can significantly improve sperm quality and fertilization outcome of frozen and chilled semen [30, 31]. Recent research has revealed that EGCG acts as a robust ROS scavenger and significantly extends boar semen storage time at 4 °C [32]. However, the inherent instability of free EGCG molecules, which are prone to oxidation or denaturation, presents a significant challenge in their therapeutic use [33, 34]. Notably, nanotechnology can transform unstable substances into stable nanomaterials, enhancing their stability, and controlled release from nanocarriers can prolong their effects [12, 14, 35]. Importantly, PDA NPs can be easily synthesized and modified to encapsulate bioactive compounds [16, 36, 37], making them suitable carriers for improving the effectiveness of EGCG in boar semen preservation.

Inspired by the dopamine ligand-receptor binding property, an attractive paradigm with the ability to activate the following cAMP/PKA signaling pathway, we introduced EGCG into the synthesis system of PDA NPs to construct polydopamine nanoparticles loaded with EGCG (EGCG@PDA NPs). This rationally designed EGCG@PDA nano-protectant will be ensuring long-time antioxidant capacity and specificity towards regulating protein phosphorylation in the preservation system of pig semen at 4 °C (Scheme 1). This study is the first to propose a novel nano-strategy to enhance boar sperm quality and reproductive performance.

## Materials and methods

### Materials

Dopamine hydrochloride (DA·HCl) and EGCG was purchased from Aladdin Reagent Co. Ltd (Shanghai, China). FITC were obtained from Sigma-Aldrich (St. Louis, MO, USA). MitoTracker® Red CMXRos staining kit were purchased from Yeasen Corporation (Shanghai, China). 4% paraformaldehyde solution, BCA protein assay kit, Triton X-100 and 4',6-diamidino-2-phenylindole (DAPI) were purchased from Beyotime (Jiangsu, China). DPPH

free radical clearance detection kit (Microplate method), Total antioxidant capacity (T-AOC) test kit (ABTS Microplate method) and D2DR antibody were purchased from Glatt Information Technology Co. Ltd (Shanghai, China) and Abcam (Cambridge, UK), respectively.

### Preparation and characterization of PDA NPs and EGCG@PDA NPs

#### Synthesis of PDA NPs

PDA NPs are synthesized following a modified method [36]. Typically, dopamine was dissolved in an aqueous solution and NaOH solution (1 M) were steadily added to facilitate the polymerization process, then the reaction mixture was stirred vigorously for 2.5 h. The produced PDA NPs were obtained by centrifugation at 11,000 × g for 20 min. Remaining contaminants were then removed using distilled water washing, and the black solids of PDA NPs were obtained by freeze-drying.

#### Synthesis of EGCG@PDA NPs

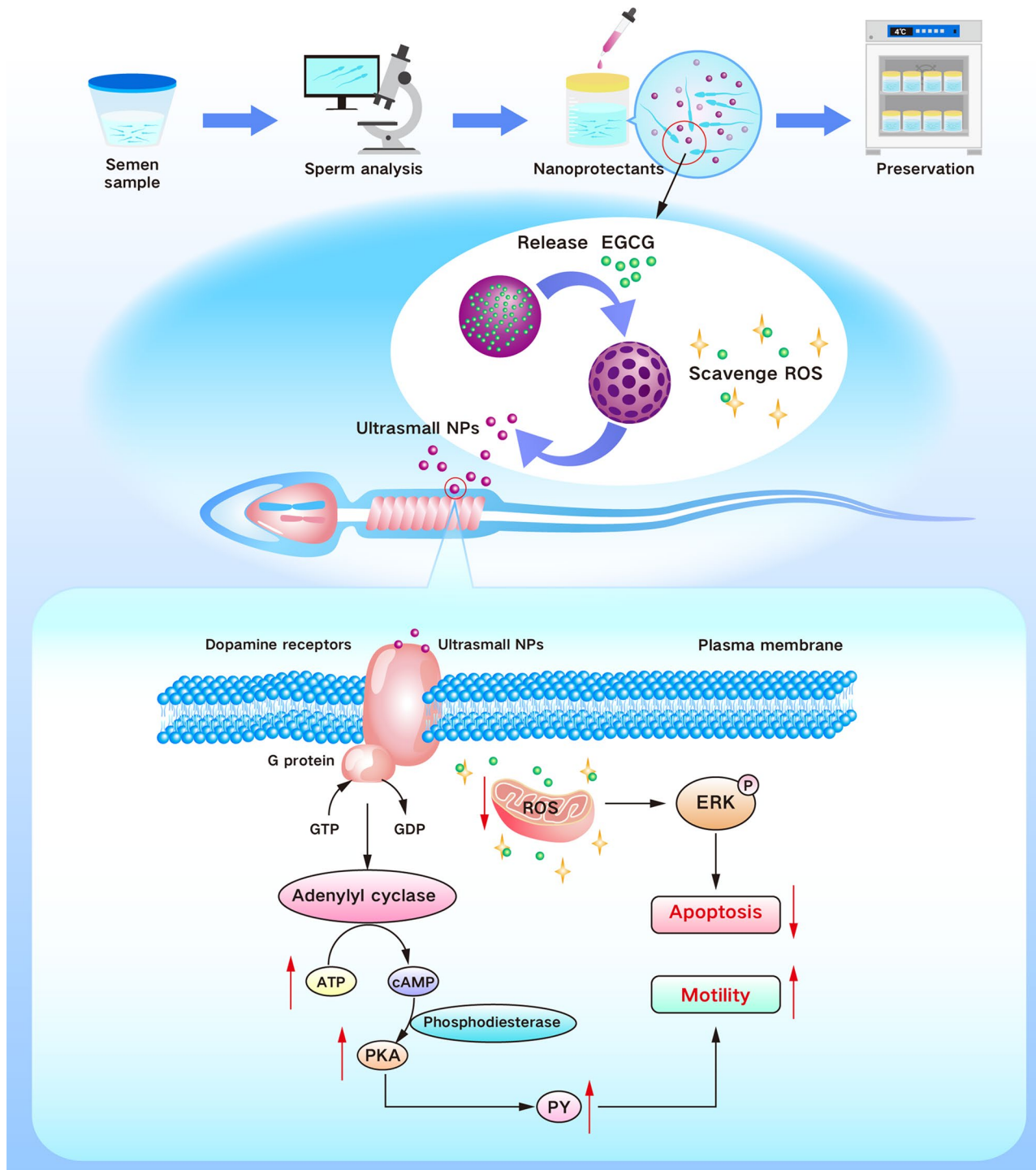
Dopamine hydrochloride (3 mg/mL) and EGCG (1 mg/mL) were dissolved in Deionized water and ethanol, respectively. Then dopamine hydrochloride solution was mixed with 1 M NaOH solution, and the mixture was vigorously stirred at 25 °C. EGCG solution was added promptly when the solution's color turned pale yellow, and the mixture ultimately turned dark brown. After centrifuging for 20 min at 12,000 × g, the EGCG@PDA NPs were collected and washed three times with deionized water to get rid of the byproduct NaCl and EGCG. Solids of EGCG@PDA NPs were obtained by freeze-drying the aqueous solvent.

#### Synthesis of FITC-EGCG@PDA NPs

FITC-labeled EGCG@PDA NPs were prepared based on the reports by Zhang et al. [38]. Briefly, DMSO solution was used to dissolve FITC. The FITC-labeled EGCG@PDA NPs were created by magnetically swirling 8 mL of EGCG@PDA NPs (1 mg/mL) with 250 µL of FITC (0.5 mg/mL) for 24 h in the dark. Then, the mixture was centrifuged at 11,000 × g for 20 min, and the pellet was washed 3 times with PBS and dialyzed with deionized water for 12 h to fully remove free FITC. FITC-labeled EGCG@PDA NPs were obtained by ultracentrifuge at 11,000 × g for 30 min and the concentration of products was evaluated by weight after lyophilization.

#### Characterization of PDA NPs and EGCG@PDA NPs

The morphological structure and size of EGCG@PDA NPs was estimated by 120 kV biological transmission electron microscopy (Hitachi, HT7700, Japan). To see the elementary of the EGCG@PDA NPs, a field emission transmission electron microscope (FE-TEM) (TAKOS, F200X, USA) was utilized. Using a Varian Cary



**Scheme 1** Schematic illustration of the mechanism by which EGCG@PDA NPs improved boar semen quality

50 spectrophotometer (Varian Inc., USA), UV-Vis spectra were captured. Utilizing Fourier-transform infrared spectroscopy (FTIR) (Bruker, Tensor 27, Germany), the chemical makeup of the EGCG@PDA NPs was examined. Using dynamic light scattering on a Nicomp 380 ZLS Zeta potential/Particle sizer (PSS Nicomp, USA), the size distribution and zeta potential were recorded.

#### Stability and degradability analysis

The stability of the EGCG@PDA NPs over time was monitored using TEM images. A dilute suspension of the NPs in deionized water was prepared to measure the size and zeta potential at regular intervals.

### DPPH radical scavenging activity

The antioxidant activity of samples was detected by DPPH radical scavenging activity [25]. PDA NPs and EGCG@PDA NPs were dispersed in deionized water and then mixed with DPPH ethanol solution following by incubation in the dark (25 °C, 30 min). Finally, an ultraviolet spectrophotometer (BIOBASE, Jinan, China) was used to test the blended solution's absorbance at 517 nm. The DPPH radical scavenging activity was calculated using the mathematic formula: DPPH scavenging activity (%) = [Abs (control) - Abs (sample)] / Abs (sample) × 100.

### ABTS scavenging activity

ABTS, a chemically stable compound, produces green cationic radicals (ABTS•<sup>+</sup>) when reacting with potassium persulfate. Antioxidative substances inhibit the formation of ABTS•<sup>+</sup>, allowing color change monitoring. An ultraviolet spectrophotometer (BIOBASE, Jinan, China) was used to measure the absorbance at 405 nm.

### Loading efficiency and loading capacity of EGCG

To get the supernatant, the nanoparticle suspensions were centrifuged for 10 min at 13,000 × g. High performance liquid chromatography (HPLC) analysis was used to determine the amount of EGCG in the supernatant. The following formulae were used to determine the loading capacity and loading efficiency:

Loading capacity = (EGCG amount loaded into nanoparticles/total nanoparticle amount) × 100%.

### Semen collection and processing

In order to evaluate sperm motility, semen samples from 15 boars were collected and sent to computer-assisted semen analysis (CASA) system (Hamilton Thorne Research, Massachusetts, USA) analysis. In this investigation, only ejaculates with motility greater than 70% were used [4, 7]. The following ingredients were included in the basic medium in which each ejaculate was diluted: 2.35 mg/ml ethylenediaminetetraacetic disodium salt, 1.0 mg/ml sodium hydrogen carbonate, 2.9 mg/ml citric acid monohydrate, 5.65 mg/ml tris (hydroxymethyl) aminomethane, 2 mg/ml skim milk, and 0.2 mg/ml amikacin sulfate are among the ingredients in 27.5 mg/ml D-fructose. The skim milk (Foodhold USA LLC, Landover, USA) was pre-processed using an ultrasonic cell crusher (Hielscher Ultrasonics GmbH, UP50H, Germany) set to sonicate it on ice for 40 min as follows: amplitude of 80% and cycle of 0.5.

In this study, four experimental groups were designed as following: Group I: 1 µg/ml, 2 µg/ml, 3 µg/ml, or 4 µg/ml of EGCG@PDANPs was supplemented in the basic medium. Subsequently, sperm motility, acrosome integrity, mitochondrial membrane potential, antioxidant ability, ATP level, and protein phosphorylation were

analyzed. Group II: DA, PDANPs, DA + PDANPs and EGCG@PDANPs (4 µg/ml) were added to the basal medium, respectively. In group II, sperm motility, acrosome integrity, mitochondrial membrane potential, antioxidant ability and ATP level were assessed. Group III: free dopamine (4 µg/ml) were added to the basal semen preservation medium and sperm motility parameters were detected. Group IV: 4 µg/ml EGCG@PDANPs was given to the basal media together with or without 30 nM raclopride, a specific D2DR antagonist. Sperm motility characteristics and sperm protein phosphorylation were measured in group IV. All the semen samples were assessed for quality in advanced and reached a final concentration of 1 × 10<sup>8</sup> cells/ml. Within 20 min, the superior semen samples were sent to the lab at 37 °C. The semen samples were moved to a sterile incubator that was kept at 4 °C. The temperature of semen samples steadily dropped to 4 °C, the ideal storage temperature, after 2 to 3 h. To avoid precipitation and guarantee homogeneity, the samples were gently shook three times a day during the incubation period.

### Assessment of sperm motility

Every sample tube was filled with 300 µl of semen, which was then incubated for 30 min at 37 °C in a water bath on the assigned experimental days (days 3, 5, 7, and 10). Next, 5 µl of every semen sample were meticulously placed onto disposable counting chamber slides that had been slightly heated beforehand (Leja, Nieuw Vennep, the Netherlands). Then sperm kinetic characteristics were quantitatively evaluated utilizing the CASA equipment. At least 200 spermatozoa were included in each sample.

### Assessment of acrosome integrity

In brief, throughout the preservation period (days 0, 3, 5, 7, and 10), the samples were centrifuged (2,000 × g, 10 min) and the pellets were suspended in PBS, supplemented with PI (1 mg/ml) to detect dead spermatozoa and PNA-FITC (100 µg/ml) to evaluate the acrosomal integrity. The samples were then incubated for 20 min in the dark at 37 °C, washed, resuspended in PBS and analyzed with flow cytometry (Beckman Coulter Ltd., Brea, USA) [39].

### Assessment of mitochondrial membrane potential (Δψ<sub>m</sub>)

To measure variations in mitochondrial membrane potential, 5,5',6,6'-tetrachloro-1,1',3,3'-tetraethylbenzimidazolyl carbocyanine iodide (JC-1) probe was utilized as a fluorescent dye [40]. Sperm cells were incubated with JC-1 dye for 0.5 h in the dark. Next, fluorescent signals were captured using flow cytometry; the FL-1 channel identified JC-1 monomers, whereas the FL-2 channel identified aggregates. FL2/FL1 was used to determine Δψ<sub>m</sub>.

### Total ROS (tROS) assay

The intracellular total ROS concentration of the semen sample was determined using the 2', 7'-dichloride-hydrofluorescein diacetate probe [41]. Semen samples collected on days 5 were re-suspended, cleaned three times in PBS, and maintained for 30 min at 37 °C in the dark using a culture solution containing DCFH-DA. The corresponding fluorescence intensity was recorded using a fluorescence spectrophotometer set to Ex/Em = 485/535 nm.

### Total antioxidative capacity (T-AOC) activity assay

The T-AOC assay kit was used to detect the T-AOC activity of boar sperm. The sperm samples were washed, centrifuged, and re-suspended with PBS for three times. Subsequently, the suspension was lysed ultrasonically on ice and centrifuged at 12,000 × g for 10 min. Then the supernatants were collected, following by the addition of reaction buffer. Finally, the value of each semen sample was recorded by a spectrophotometer at 520 nm [42], and corresponding T-AOC activity of each sample was calculated and expressed as U/ml.

### Malondialdehyde (MDA) content assay

MDA content was measured according to the manufacturer's protocol [4]. Semen was collected and sperm were lysed in ice-cold lysis buffer containing 50 mM Tris-HCl (pH 7.5), 5 mM EDTA, and 1 mM DTT by sonication on several preserved time points. After that, the lysed solution was centrifuged to get rid of the unlysed cell debris. Lastly, a spectrophotometer was used to determine the absorbance at 532 nm.

### Measurement of ATP content

An ATP test kit for bioluminescence was used to measure the quantities of ATP [43, 44]. In detail, samples were centrifuged and washed twice with PBS. Subsequently, lysis buffer was incubated with the sperm pellets to extract intracellular ATP. Then the extracts were mixed with luciferase reagent and corresponding fluorescent signals were captured using an illuminometer. Meanwhile, the ATP standard curve was also prepared via mixing serial dilutions of the ATP standard solution with luciferase reagent to generate bioluminescence signals.

### SDS-PAGE and immunoblotting

Samples of semen were collected and centrifuged for 5 min at 12,500 ×g. The proteins were then extracted using protein lysis buffer and measured using the BCA protein kit (Beyotime Institute of Biotechnology, Nanjing, China). After SDS-PAGE resolution and polyvinylidene fluoride (PVDF) membrane transfer, membranes were blocked using bull serum albumin (BSA), following by immunoblotting with either anti-phosphotyrosine antibody (Millipore, Boston, USA, Cat# 05-321, clone

4G10) or anti-P-PKA antibody (Cell Signaling Technology, Danvers, USA, Cat# 9624, clone 100G7E). An enhanced chemiluminescence ECL-plus kit (Thermo Scientific, Waltham, USA) was used to detect signals, and a ChemiScope 3300 small integrated chemiluminescence imaging system (Clinx, Shanghai) was used to record the signals. The molecular weights of sperm proteins are expressed as kDa [45].

### Immunofluorescence

Samples of semen were collected, centrifuged and then suspended in PBS solution. They were then put on slides and air-dried for 30 min. Subsequently, they underwent formaldehyde fixation, Triton X-100 permeabilization, washing, BSA blocking, and an overnight incubation with either anti-phosphotyrosine antibody or anti-P-PKA antibody at 4 °C. Sperm were incubated for 2 h at room temperature using Alexa 555-conjugated anti-rabbit antibody or Alexa 488-conjugated anti-mouse antibody, along with Alexa 555-conjugated PNA (Molecular Probes, Cat# L-21409) (1:100) for staining acrosomes and DAPI (Jianglai biology, Shanghai, JL-RDA50) (1:100) for sperm nuclei detection. Ultimately, the sperm were cleaned, placed on slides and studied with a 400 × objective under a confocal fluorescence microscope (Leica, Wetzlar, Germany) [7].

### Biocompatibility and safety evaluation of EGCG@PDA NPs

As EGCG@PDA NPs will finally degrade into free EGCG and dopamine (DA) molecules, sperm motility parameters were evaluated in free DA-treated group to evaluate the safety of EGCG@PDA NPs.

### Electron microscopy of boar sperm

After preserved with EGCG@PDA NPs for 5 days, sperm were collected and immersed in 2.5% glutaraldehyde at 4 °C. After dehydration and embedding, ultrathin sections were prepared. Next, lead citrate and uranyl acetate were used to stain the sections. Using a transmission electron microscope, the ultrastructure of spermatozoa was examined (TEM, HT7700, HITACHI, Tokyo, Japan) [12].

### Statistical analysis

The statistical program SPSS 22.6 (SPSS Incorporated, Armonk, USA) was used to analyze all the data. Every experiment was run at least three times, and the quantitative results were shown as mean ± standard deviation (SD). Turkey's multiple comparison tests, one-way and two-way ANOVA analyses, and other statistical methods were used to assess the significance of the difference. Significant and highly significant values were set at  $P < 0.05$  and  $P < 0.01$ , respectively.

## Results

### Synthesis and characterization of EGCG@PDA nanoparticles

Firstly, we constructed an environmentally-friendly size-adjustable synthesis approach to make PDA nanoparticles with diameters ranging from 100 nm to 400 nm, allowing for the tailored fabrication of nanoparticles with desired diameters (Fig. 1S). More hydroxide ions ( $\text{OH}^-$ )

will significantly speed up the dopamine (DA) polymerization kinetics through self-oxidative polymerization in an alkaline medium, resulting in smaller-diameter PDA nanoparticles (Fig. 1S). Using a similar approach, EGCG@PDA nanoparticles with different diameters were fabricated using DA and EGCG as building blocks (Fig. 1A). The morphology of EGCG@PDA NPs was investigated by transmission electron microscopy (TEM)

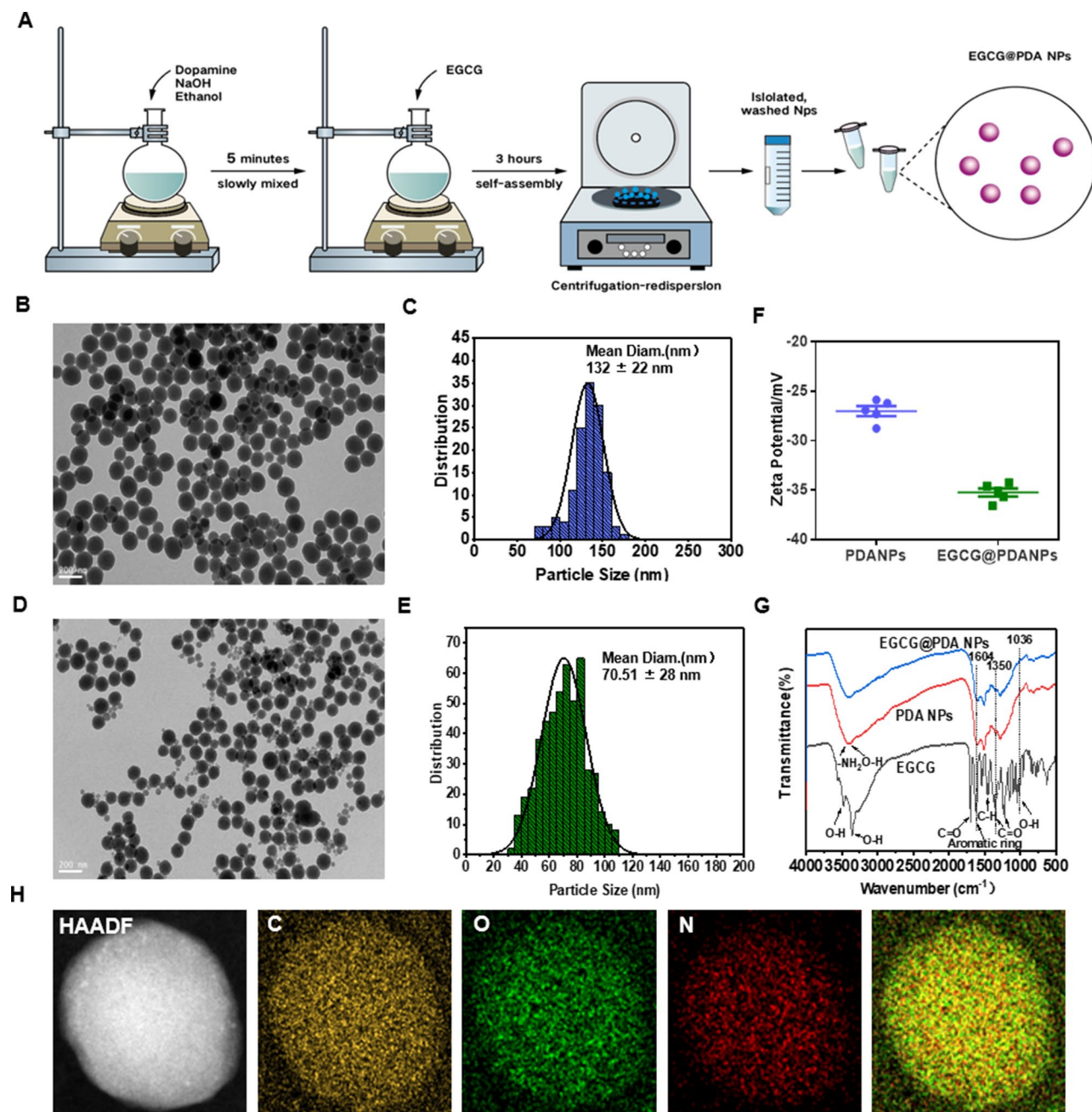


**Fig. 1** The synthesis and characterization of EGCG@PDANPs. **(A)** The synthesis schematic of EGCG@PDANPs. **(B)** The transmission electron microscopy image of PDANPs. **(C)** The particle size distribution of PDANPs. **(D)** The transmission electron microscopy image of EGCG@PDANPs. **(E)** The particle size distribution of EGCG@PDANPs. **(F)** The zeta potential of PDANPs and EGCG@PDANPs. **(G)** The infrared spectrum of EGCG, PDANPs and EGCG@PDANPs. **(H)** The mapping of the elements C, O, and N in EGCG@PDANPs

and dynamic light scattering (DLS) analysis (Fig. S3). As presented in Fig. 1D and Fig. S3, EGCG@PDA NPs displayed excellent dispersal and uniform spherical shapes with minimal aggregations. This might be contributed to the structural characteristics of EGCG, which may guide the  $\pi$ - $\pi$  supramolecular interactions and prevent the stacking of polydopamine molecules [46–48]. Furthermore, the zeta potential and EGCG loading efficiency of these hybrid nanoparticles were evaluated (Fig. S4 and S5). The zeta potentials of PDA NPs and EGCG@PDA NPs were  $-27\text{mV}$  and  $-35.2\text{mV}$ , respectively (Fig. 1F), suggesting their high colloidal stability. Subsequently, we optimized the blending ratios to explore their influence on the antioxidant capacity (Fig. S2 and Fig. S6), founding that smaller nanoparticles exhibited stronger antioxidant capacity, likely due to their larger specific surface areas [49]. It is widely accepted that smaller particles are more efficient at diffusing throughout media and penetrating through cell membranes [50, 51]. Consequently, we selected a blending ratio featuring  $\sim 70\text{ nm}$  EGCG@PDA NPs for subsequent experiment. Infrared spectroscopy was also employed to analyze the resonance patterns of diverse functional groups, comparing these patterns with the spectra of EGCG and PDA to confirm the successful encapsulation of EGCG within the PDA NPs (Fig. 1G). The elemental composition and structure of the nanoparticles were further ascertained through element mapping assay (Fig. 1H). Conclusively, in this research, EGCG@PDA nanoparticles were effectively fabricated using a facile method.

#### The antioxidant capability and stability of EGCG@PDA NPs

The antioxidant capabilities of EGCG@PDA NPs, PDA NPs, and EGCG in aqueous solutions were evaluated (Fig. 2A–D). The DPPH radical scavenging activity and ABST total antioxidant capacity assays indicated that, under identical concentration conditions ( $6\text{--}12\ \mu\text{g/ml}$ ), EGCG@PDA NPs exhibited the most sustained antioxidant capacity, with a slow decline throughout the duration of the *in vitro* preservation experiment. In contrast, both PDA NPs and EGCG demonstrated a significant decrease in antioxidant capacity on the fifth day of *in vitro* preservation.

Morphological stability of PDA NPs and EGCG@PDA NPs in aqueous solution over time is depicted in Fig. S7. On day 0 of *ex vivo* storage, both types of nanoparticles maintained their original structures. This stability remained until day 7, indicating their robustness in aqueous solution (Fig. S7). To further assess the stability of EGCG@PDA NPs in biological environments, they were stored separately in semen and  $\text{H}_2\text{O}_2$  solutions for 7 days. Transmission electron microscopy results showed that with increasing storage time, EGCG@PDA NPs gradually degraded into ultra-small particles less than  $10\text{ nm}$

in semen, while the degradation rate was faster in  $\text{H}_2\text{O}_2$  solution (Fig. 2E, Fig. S8 and Fig. S9).

#### EGCG@PDA NPs improve boar sperm quality parameters

Results depicted in Fig. 3A–C indicate that doses of 1, 2, 3, and  $4\ \mu\text{g/ml}$  of EGCG@PDA NPs significantly enhanced sperm motility parameters compared to the control. Notably, the group receiving  $4\ \mu\text{g/ml}$  of EGCG@PDA NPs displayed the highest motility. Throughout the storage period, treatment groups consistently displayed increased levels of both progressive motility (PRO) and total motility (MOT) in a dose-dependent manner compared to the control group ( $P < 0.05$ ) (Fig. 3A–F).

The percentage of viable spermatozoa with intact acrosomes in the EGCG@PDA NPs-treated group demonstrated potential dose-dependent effects when comparing with that in the untreated group (Fig. 3G–I). Additionally, during the entire experimental period, the  $4\ \mu\text{g/ml}$  EGCG@PDA NPs-treated group outperformed the  $2\ \mu\text{g/ml}$  and  $3\ \mu\text{g/ml}$  treated groups in terms of acrosome integrity ( $P < 0.05$ ). In summary, supplementation with  $4\ \mu\text{g/ml}$  of EGCG@PDA NPs demonstrated the most protective effects on sperm acrosomes.

Following a 10-day preservation period (Fig. 3J–L), Mitochondrial membrane potential ( $\Delta\psi\text{m}$ ) significantly increased in a concentration-dependent manner in the treatment groups compared to the control group ( $P < 0.05$  or  $P < 0.01$ ). Furthermore, boar sperm treated with  $3\ \mu\text{g/ml}$  and  $4\ \mu\text{g/ml}$  EGCG@PDA NPs exhibited higher  $\Delta\psi\text{m}$  than those treated with  $1\ \mu\text{g/ml}$  and  $2\ \mu\text{g/ml}$  EGCG@PDA NPs ( $P < 0.01$ ), with no statistically significant difference observed between the latter two dose groups.

Further results disclosed that the control group showed the lowest ATP levels across all groups as *in vitro* storage time increased ( $P < 0.05$ ) (Fig. S10), which was in line with the observed declines in sperm motility and  $\Delta\psi\text{m}$ . Moreover, both the  $3\ \mu\text{g/ml}$  and  $4\ \mu\text{g/ml}$  treatment groups manifested higher ATP levels, with no significant difference between them. In conclusion, EGCG@PDA NPs supplementation markedly protected sperm quality parameters and extended semen preservation up to 10 days.

#### The superiority of EGCG@PDA NPs in improving boar semen quality

Next, the protective effects of free EGCG, PDA NPs, a mixture of EGCG/PDA NPs and EGCG@PDA NPs against boar sperm were evaluated over the preservation durations of 5, 7 and 10 days. Sperm motility parameters for free EGCG, PDA NPs, EGCG/PDA NPs mixture and EGCG@PDA NPs were recorded, respectively. Notably, both the nanoparticles and the mixture group exhibited superior motility parameters than the free formulations

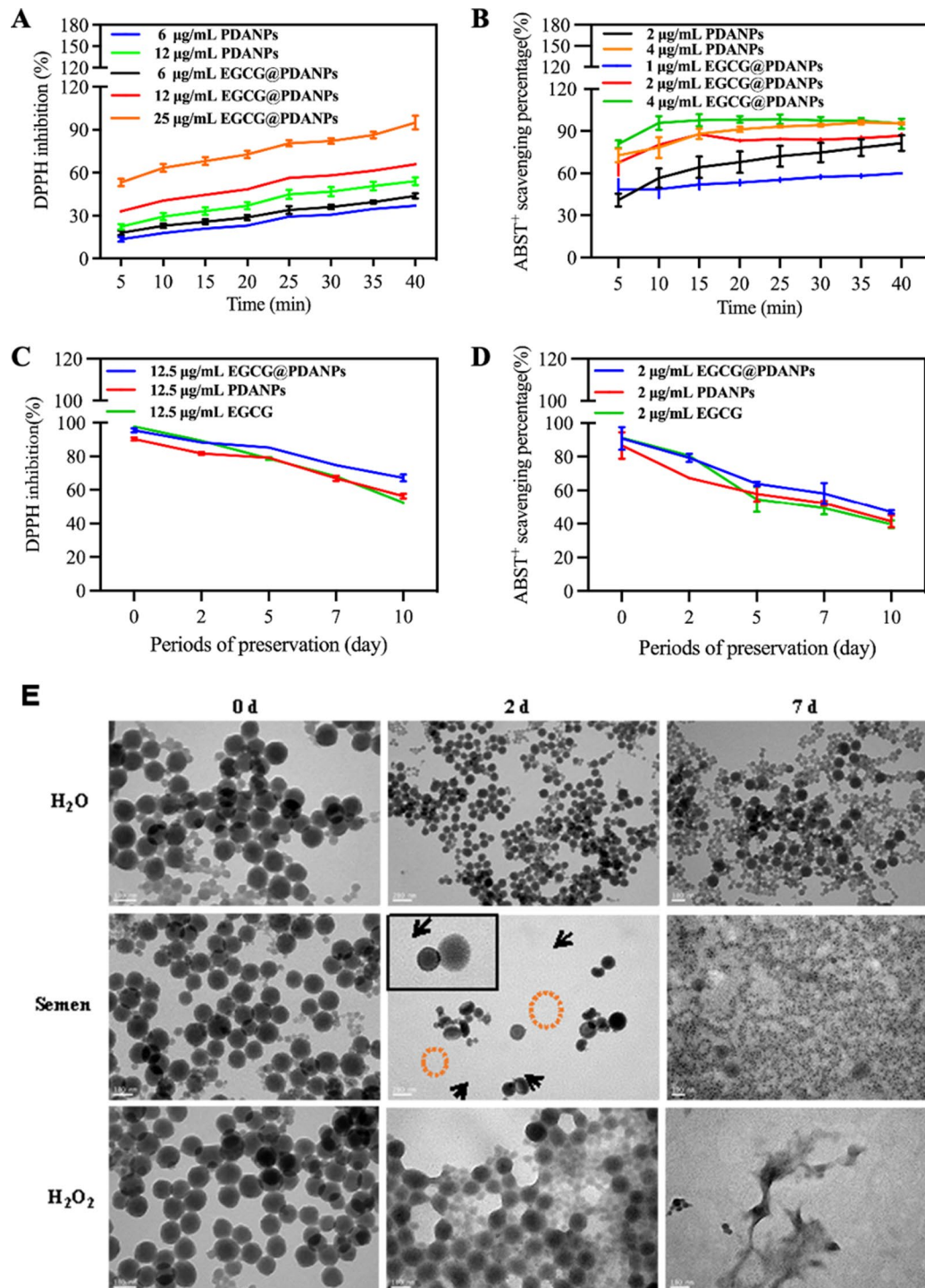


**Fig. 2** (A) DPPH inhibition rate of EGCG@PDA NPs and PDA NPs under different determination times. (B) ABST<sup>+</sup> scavenging ability of EGCG@PDA NPs and PDA NPs in vitro under different determination times. (C) DPPH scavenging ability of EGCG@PDA NPs and PDA NPs at different concentrations and under different storage days. (D) Total antioxidant capacity of EGCG@PDA NPs and PDA NPs at different concentrations and under different storage days. (E) The stability of EGCG@PDA NPs under water solutions and the degradability of EGCG@PDA NPs under semen or H<sub>2</sub>O<sub>2</sub> systems

(Tables 1 and 2), indicating a robust synergistic impact on enhancing sperm quality.

During the preservation period, the percentage of acrosome integrity in the EGCG@PDA NPs-treated group

exceeded that of the other three formulations (Fig. 4A-C). Similarly, data analysis of mitochondrial membrane potential and ATP levels throughout the preservation period showed that EGCG@PDA NPs possess great

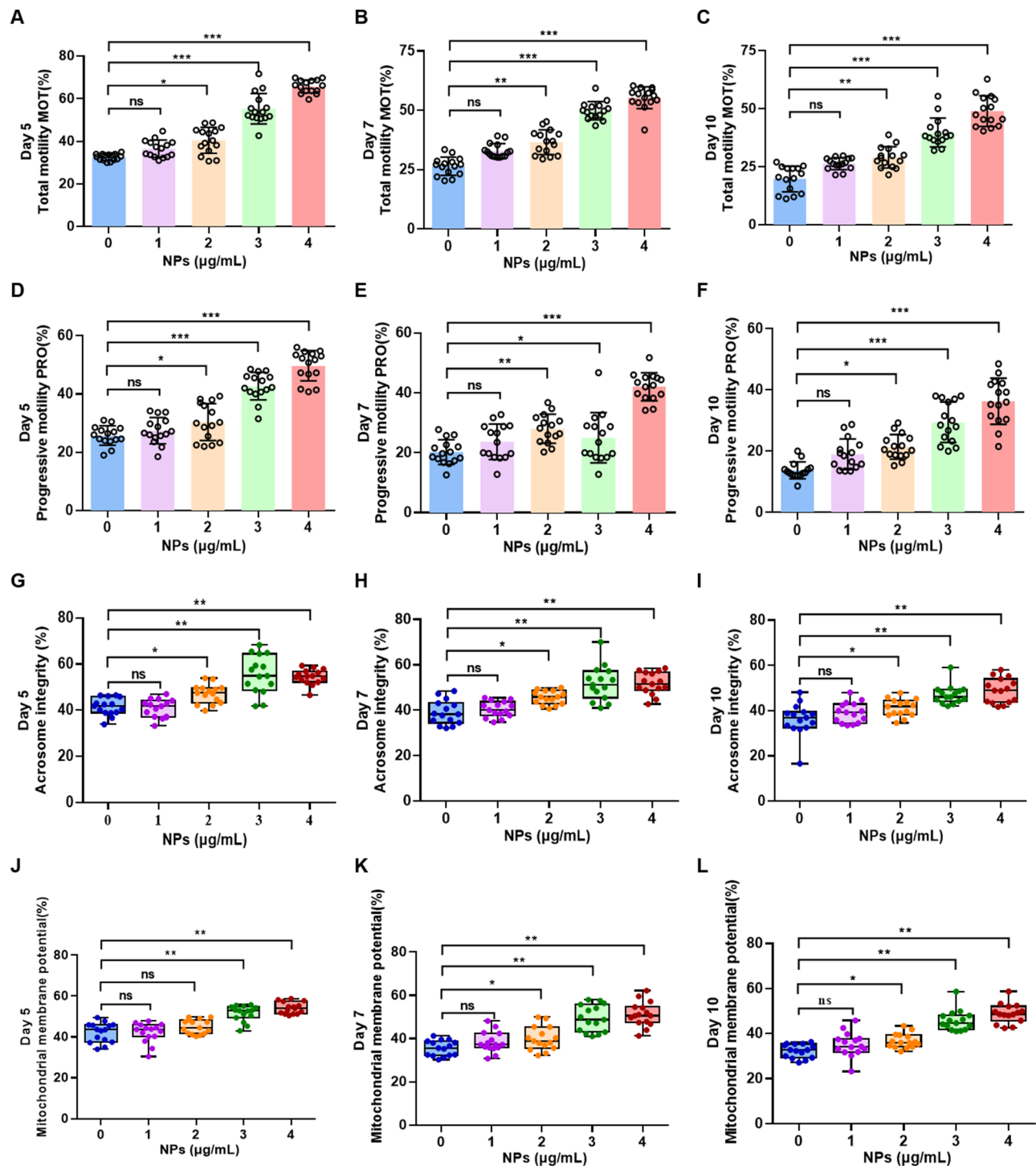


**Fig. 3** Effects of different concentrations of EGCG@PDANPs on sperm quality parameters. Total sperm motility at Day 5 (A), Day 7 (B) and Day 10 (C). Progressive motility at Day 5 (D), Day 7 (E) and Day 10 (F). Acrosome integrity at Day 5 (G), Day 7 (H) and Day 10 (I). Mitochondrial membrane potential at Day 5 (J), Day 7 (K) and Day 10 (L). ( $n = 15$ ,  $P < 0.05$ )

superiority in comparison with the other formulations (Fig. 4D-G).

In addition, as EGCG@PDA NPs would ultimately degrade into free EGCG and dopamine (DA) molecules, the safety of EGCG@PDA NPs as an alternative

protective agent was comprehensively assessed using the same dose of DA (4 µg/ml). The effects of the DA on the vitality parameters of low-temperature preserved pig sperm were shown in Fig. 4H-I and Fig. S11. As the preservation time increased, both the control and DA

**Table 1** Effects of different treatments on sperm total motility (MOT) during the preservation period

MOT (%)	3 day	5 day	7 day	10 day
Control	43.11 ± 4.44 <sup>b</sup>	42.56 ± 4.47 <sup>b</sup>	38.85 ± 5.42 <sup>b</sup>	38.77 ± 5.25 <sup>b</sup>
EGCG	35.47 ± 5.26 <sup>a</sup>	33.58 ± 7.25 <sup>a</sup>	26.75 ± 5.91 <sup>a</sup>	25.30 ± 5.68 <sup>a</sup>
PDA	36.50 ± 6.11 <sup>a</sup>	36.61 ± 9.31 <sup>a</sup>	26.56 ± 4.62 <sup>a</sup>	27.23 ± 5.10 <sup>a</sup>
EGCG + PDA	44.56 ± 6.20 <sup>b</sup>	40.75 ± 6.17 <sup>b</sup>	38.77 ± 4.16 <sup>b</sup>	35.80 ± 5.52 <sup>b</sup>
NPs	58.58 ± 5.85 <sup>c</sup>	59.96 ± 7.60 <sup>c</sup>	53.72 ± 6.67 <sup>c</sup>	58.77 ± 5.24 <sup>c</sup>

Data are presented as mean ± standard deviation from fifteen replicated experiments. Values with different superscript letters differed significantly ( $P < 0.05$ )

**Table 2** Effects of different treatments on sperm progressive motility (PRO) at different preservation times

PRO (%)	3 day	5 day	7 day	10 day
Control	26.22 ± 4.77 <sup>b</sup>	25.18 ± 4.10 <sup>b</sup>	22.54 ± 4.10 <sup>b</sup>	22.75 ± 4.53 <sup>b</sup>
EGCG	19.95 ± 4.04 <sup>a</sup>	19.62 ± 6.67 <sup>a</sup>	14.44 ± 3.32 <sup>a</sup>	13.71 ± 3.56 <sup>a</sup>
PDA	20.99 ± 6.30 <sup>a</sup>	22.24 ± 7.21 <sup>a</sup>	14.58 ± 2.40 <sup>a</sup>	15.14 ± 2.76 <sup>a</sup>
EGCG + PDA	26.28 ± 4.33 <sup>b</sup>	23.97 ± 5.58 <sup>b</sup>	22.07 ± 4.56 <sup>a</sup>	20.02 ± 4.62 <sup>b</sup>
NPs	35.71 ± 6.59 <sup>c</sup>	37.87 ± 6.42 <sup>c</sup>	30.12 ± 6.41 <sup>c</sup>	34.85 ± 6.11 <sup>c</sup>

Data are presented as mean ± standard deviation from fifteen replicated experiments. Values with different superscript letters differed significantly ( $P < 0.05$ )

treatment groups (4 µg/ml) showed a decline in sperm vitality. However, at different preservation time points, the sperm motility of DA-treated group was markedly higher compared with that of the control group ( $p < 0.05$ ). As shown in Fig. 4H-I, the changes in the progressive motility index of sperm were similar to the changes in sperm total motility ( $P < 0.05$ ). These results illustrate that treatment with 4 µg/ml DA does not exert toxic effects on low-temperature preserved pig sperm and can improve sperm vitality, suggesting the good biocompatibility and safety of EGCG@PDA NPs for use in boar semen preservation.

#### EGCG@PDA NPs enhance antioxidant ability of boar sperm and prevent sperm apoptosis via ERK signaling pathway.

Moreover, the potential effects of EGCG@PDA NPs on the antioxidant ability of boar sperm were investigated. The results revealed that EGCG@PDA NPs significantly enhanced the antioxidant ability of boar sperm, as evidenced by the increased total antioxidant capability (T-AOC) and reduced levels of ROS and MDA content in the treated group compared to the control group (Fig. 5A-C). Specifically, EGCG@PDA NPs exhibited superior ROS scavenging capacity compared to free EGCG or PDA NPs (Fig. 5D-F), highlighting the advantage of EGCG@PDA NPs in antioxidative performance during boar semen preservation.

Remarkably, supplementation with EGCG@PDA NPs activated the ERK signaling pathway, as manifested by the augmented phosphorylation of ERK1/2 (Fig. 5G-H), suggesting that the ERK signaling pathway might be involved in the anti-oxidation and anti-apoptotic effects

of EGCG@PDA NPs on boar sperm. In conclusion, our study highlights the superior antioxidative performance of EGCG@PDA NPs compared to free EGCG or PDA NPs during boar semen preservation. Further, supplementation with EGCG@PDA NPs enhances boar sperm antioxidant ability and prevents apoptosis via the activation of the ERK signaling pathway (Fig. 5I).

#### EGCG@PDA NPs promote protein phosphorylation via D2DR-mediated cAMP/PKA signaling pathway

Intriguingly, the current study further explored the effect of varying concentrations of EGCG@PDA NPs on protein phosphorylation in boar sperm. The results revealed that the phosphorylation levels of PKA substrates (P-PKAs) were markedly higher in the treatment groups in contrast to the control group ( $P < 0.05$ ) (Fig. 6A, B). Briefly, treatment with 2, 3, and 4 µg/ml EGCG@PDA NPs resulted in significantly enhanced P-PKAs compared to the control group. Notably, supplementation with 3 µg/ml EGCG@PDA NPs exhibited the most pronounced increase in P-PKAs levels compared to the other treatment groups ( $P < 0.05$ ) (Fig. 6A-B). Similarly, EGCG@PDA NPs also enhanced tyrosine phosphorylation (PTP) levels, with the most substantial increase observed in sperm preserved with 3 and 4 µg/ml EGCG@PDA NPs ( $P < 0.05$ ) (Fig. 6C-D). Collectively, the above findings suggest that the optimal dosage of EGCG@PDA NPs for enhancing protein phosphorylation in boar sperm is 3 µg/ml or 4 µg/ml. Additionally, immunolocalization analysis of PKA substrate-phosphorylated and tyrosine-phosphorylated proteins in boar sperm further confirmed the stimulatory effect of EGCG@PDA NPs on protein phosphorylation, consistent with the western blot results (Fig. 6E-F).

Another western blot analysis revealed a specific band around 51 kDa (Fig. 7A), which corresponds to the molecular size of D2DR and is comparable to mouse sperm samples (positive control). Immunofluorescence staining exhibited the highest level of D2DR immunoreactivity in the midpiece of boar sperm (Fig. 7B). To further clarify the regulatory role of D2DR in EGCG@PDA NPs-promoted protein phosphorylation, the changes of P-PKAs and PTP in the 4 µg/ml EGCG@PDA NPs treatment group with or without raclopride, a specific D2DR antagonist, were analyzed. As demonstrated in Fig. 7C-E, lower levels of P-PKAs and PTPs were observed in the EGCG@PDA NPs + raclopride treatment group after the same preservation period. Interestingly, total motility and progressive motility decreased substantially when raclopride was co-treated (Fig. 7G-I), which may be due to blockade of D2DR by raclopride. Therefore, our results indicate that EGCG@PDA NPs affect protein phosphorylation, at least partially, through the D2DR-mediated cAMP/PKA signaling pathway (Fig. 7J).

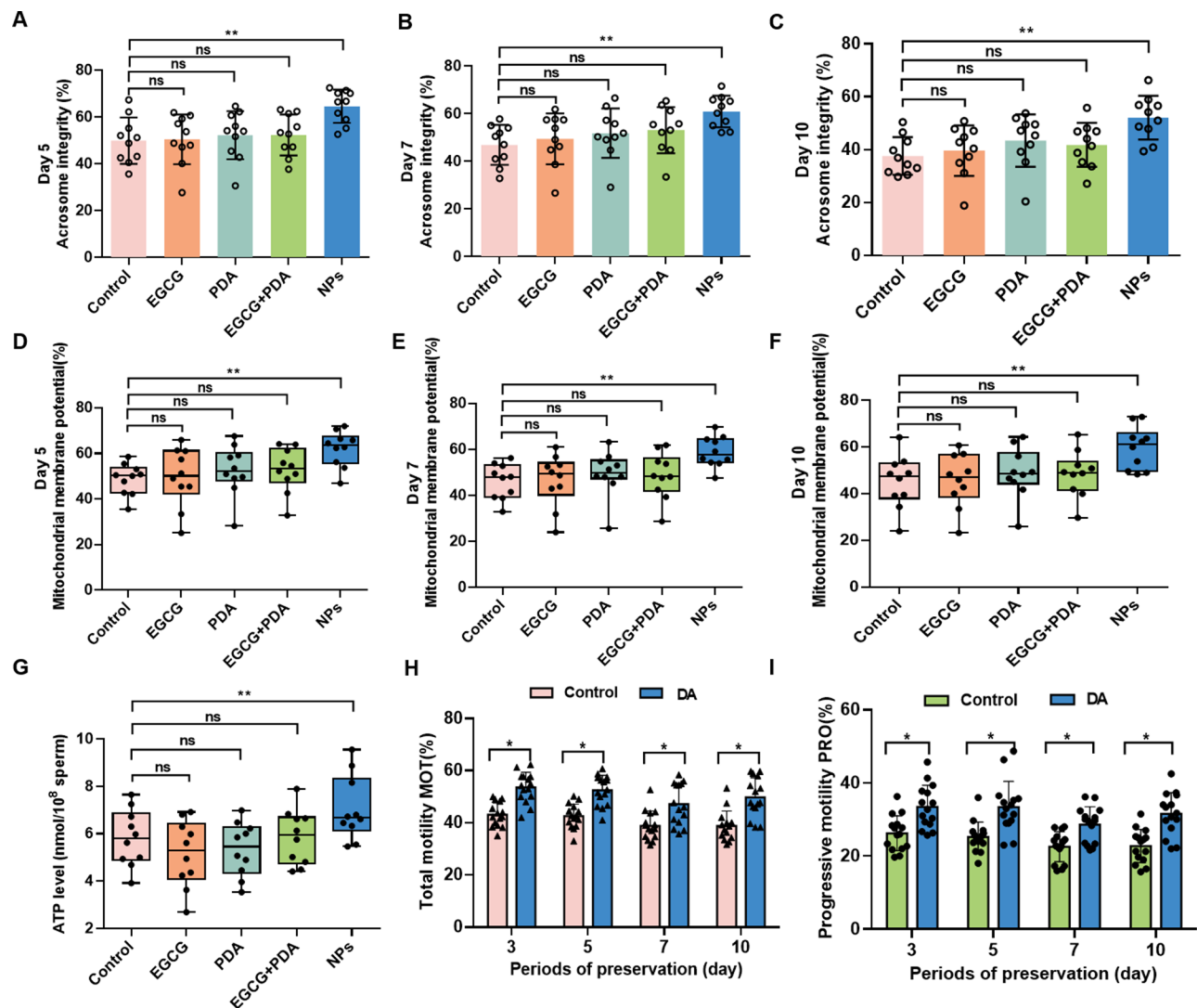


**Fig. 4** The superiority of EGCG@PDA NPs in improving boar semen quality. (A–C) The change of acrosome integrity at different preservation times. (D–F) The change of Mitochondrial membrane potential at different preservation times. ( $n = 10$ ,  $P < 0.05$ ) (G) ATP levels of sperm under different treatment conditions on day 5. (H–I) Effects of storage time and DA on motility parameters of boar sperm. ( $n = 10$ ,  $P < 0.05$ )

### Interactions of EGCG@PDA NPs with sperm

To explore the interaction of EGCG@PDA NPs with sperm cells, the cellular uptake of nanoparticles was detected via confocal laser scanning microscopy (CLSM) and flow cytometry. Fluorescein isothiocyanate (FITC), a fluorescent probe, was used to label the EGCG@PDA NPs to track the uptake efficiency of the nanostructures. Flow cytometry results showed that the fluorescence intensity of sperm treated with FITC-labelled NPs increased time-dependently (Fig. S12), indicating the cellular adhesion or uptake of EGCG@PDA NPs. To further distinguish whether the fluorescence signal was primarily contributed by internalized or membrane-absorbed NPs, CLSM images revealed that the fluorescence intensity were mainly localized in the midpiece of sperm and rapidly increased in intensity as incubation time increased

(Fig. 8A). However, it cannot be distinguished whether EGCG@PDA NPs entered the sperm cells. Meanwhile, to confirm the interaction of EGCG@PDA NPs with boar sperm, samples were observed with TEM. Ultrasmall EGCG@PDA NPs nanoparticles, either as aggregates or single nanoparticles, were found attached to the plasma membrane of boar sperm (especially in the midpiece region) or dispersed in the semen (Fig. 8B), which is inconsistent with the CLSM results and provided no evidence for the internalization of EGCG@PDA NPs into sperm cells.

Inspiringly, since D2DR is primarily located in the mid-piece of boar sperm and is a transmembrane receptor, we performed molecular docking simulations between dopamine and D2DR. As presented in Fig. 8C, the dopamine binds to the surface of the active pocket of D2DR, where

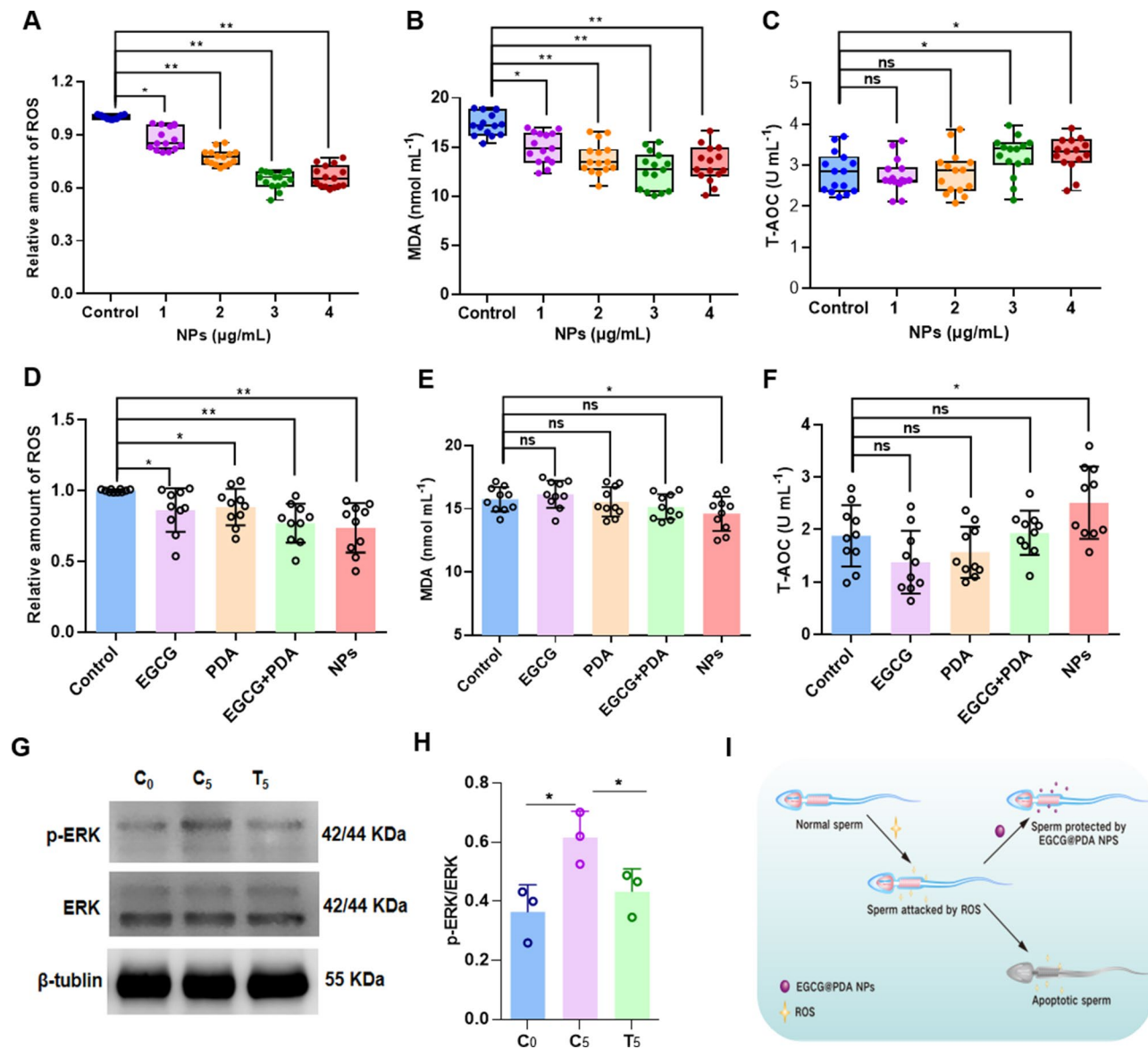


**Fig. 5** Effects of different concentrations of EGCG@PDANPs on total ROS content (**A**), MDA content (**B**) and T-AOC (**C**). Effects of different treatment groups on total ROS content (**D**), MDA content (**E**) and T-AOC (**F**) ( $n=10$ ,  $P<0.05$ ). (**G**) Western blot of ERK and p-ERK and relative amount analysis (**H**). (**I**) schematic illustration of the inhibition of EGCG@PDANPs on sperm apoptosis

residues CYS130, VAL127, TRP398, PHE401, PHE402 and others contributing to hydrophobic interactions with dopamine. The ligand forms hydrogen bonds with residue SER205 of D2DR, along with a hydrogen bond and a salt bridge with residue ASP126. Additionally, it forms a  $\pi$ -cation ( $\pi$ -cationic) interaction with residue PHE401 and a  $\pi$ - $\pi$  interaction with residue PHE402. Taken together, we hypothesize that the attachment of EGCG@PDA NPs to sperm may trigger D2DR-mediated cAMP/PKA signaling pathway, thereby enhancing p-PKAs and PTP and ultimately improving sperm motility.

## Discussion

Extensive research has highlighted the importance of protectants and additives in maintaining sperm quality during the hypothermic liquid storage of semen. Drawn from previous researches, oxidative damage and decreased sperm protein phosphorylation levels act as two main challenges influencing boar semen quality during hypothermic liquid preservation [4, 52], making them ideal targets for improving semen quality. Further investigations are required to identify optimal protectants and additives that can extend the preservation period of boar semen.

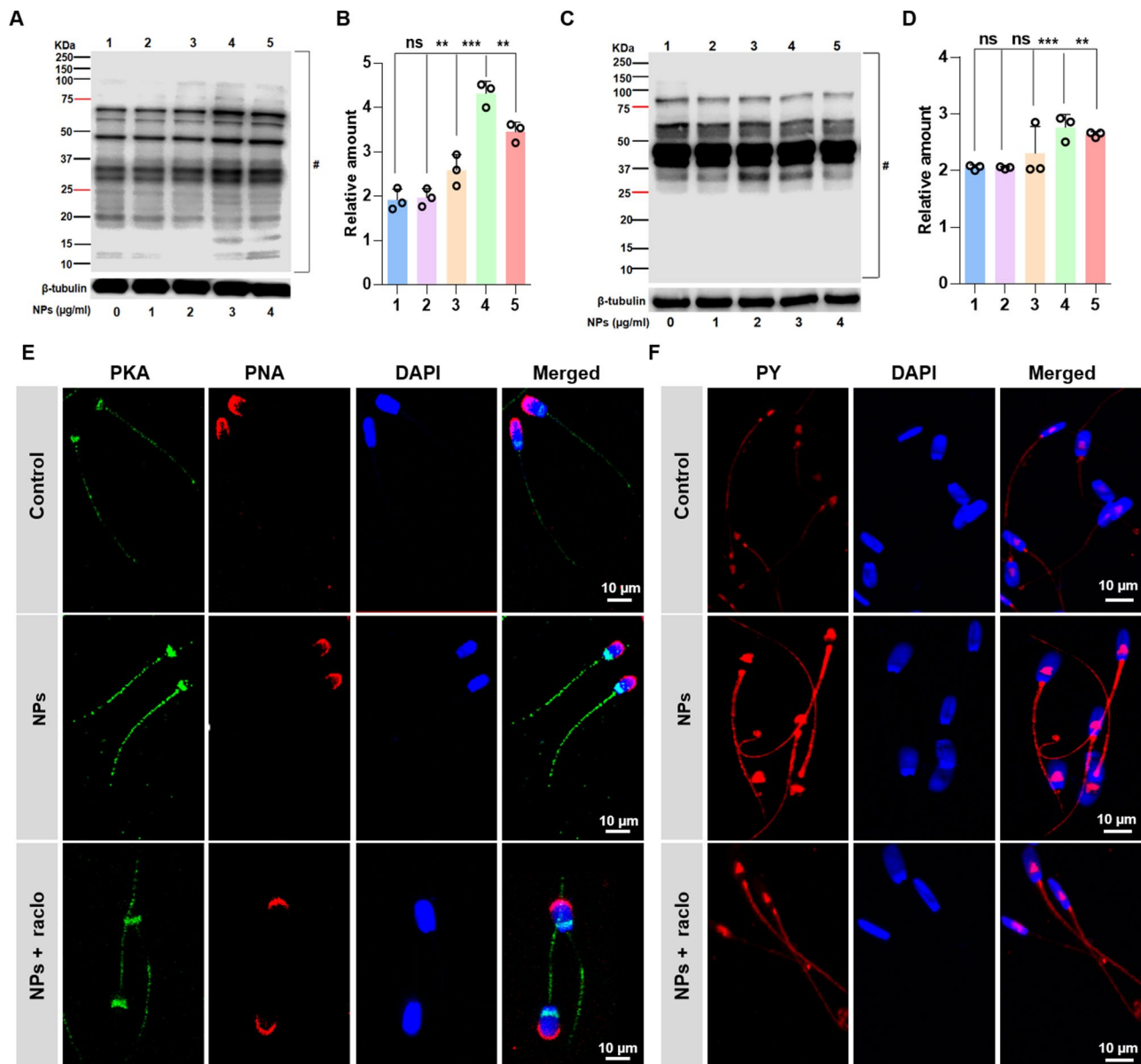


**Fig. 6** Effects of different concentrations of EGCG@PDA NPs on protein phosphorylation levels. WB results and quantitative analysis of sperm all-protein P-PKAs (**A, B**), and PY (**C, D**) in control and different EGCG@PDA NPs treatment groups on Day 5. ( $n = 3, P < 0.05$ ) (**E, F**) Immunofluorescence localization of P-PKAs and PTP in sperm cells under different treatment groups. Sperm cells were observed with a confocal laser scanning microscope ( $\times 400$ )

In this study, we aimed to develop a novel dual protective strategy targeting ROS-induced damage and reduced protein phosphorylation by constructing ROS-responsive polydopamine nanoparticles loaded with EGCG (EGCG@PDA NPs) (Fig. 1). Our findings demonstrate the potential of these nanoparticles as an effective nanoprotectant for prolonging sperm survival, owing to their synergistic effect to scavenge ROS and upregulate protein phosphorylation through the activation of D2DR/cAMP/PKA signaling pathway in boar sperm. One of the primary findings of this study is that 4 µg/mL EGCG@PDA NPs significantly extended the preservation period

from 3 days to 10 days, as evidenced by improvements in sperm motility parameters, acrosome integrity, mitochondrial membrane potential and ATP levels (Figs. 3 and 4). Notably, the effective dose of our proposed nanoprotectant in the present study was relatively lower in contrast to the previous studies on boar semen preservation [7, 53], which may be attributed to the differences of species and preservation methods, further indicating the superior protective effects of our nanoprotectant.

Abundant evidence demonstrates that sperm motility, viability, and morphology are all adversely affected by excessive ROS production [54, 55], suggesting the

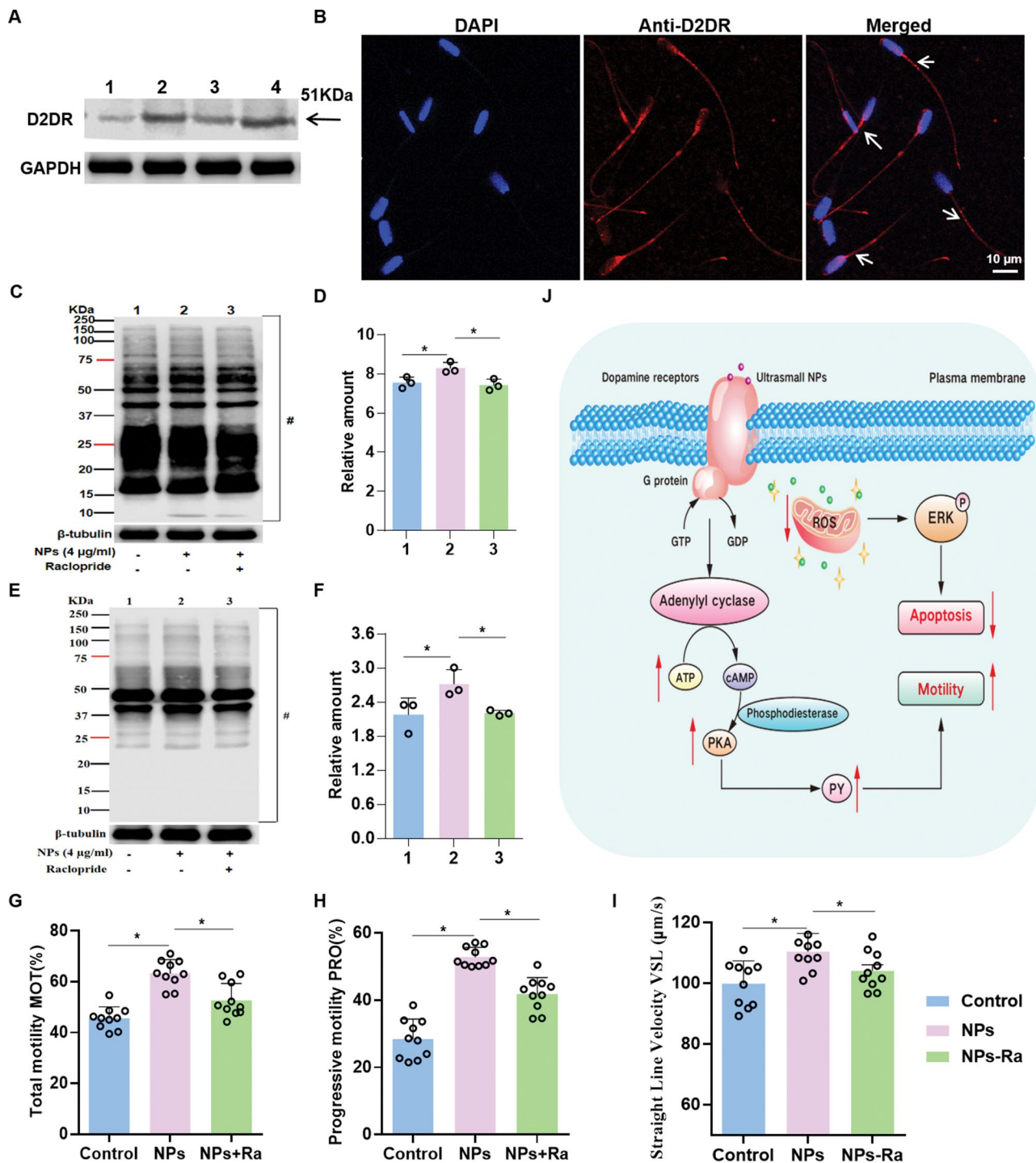


**Fig. 7** Verification of D2DR in EGCG@PDA NPs induced protein phosphorylation. A and B are WB results and immunofluorescence localization of boar sperm membrane D2DR receptor; C and D represent the effects of raclopride and EGCG@PDA NPs treatment on P-PKA; E and F represent the effects of raclopride and EGCG@PDA NPs treatment on PTP; G, H, and I represent the effects of raclopride and EGCG@PDA NPs treatment on sperm motility parameters. ( $n = 10, P < 0.05$ ); J is the proposed schematic of D2DR-mediated regulation mechanism of protein phosphorylation

negative relationship between ROS levels and sperm quality. In this regard, EGCG@PDA NPs has also been validated as a beneficial antioxidant for sperm storage at 4 °C, supported by the enhancing antioxidative

capacity and reducing intracellular ROS and MDA levels (Fig. 5), which was inconsistent with earlier studies [4, 6]. Remarkably, EGCG@PDA NPs exhibited the strongest protective effect on boar semen compared with

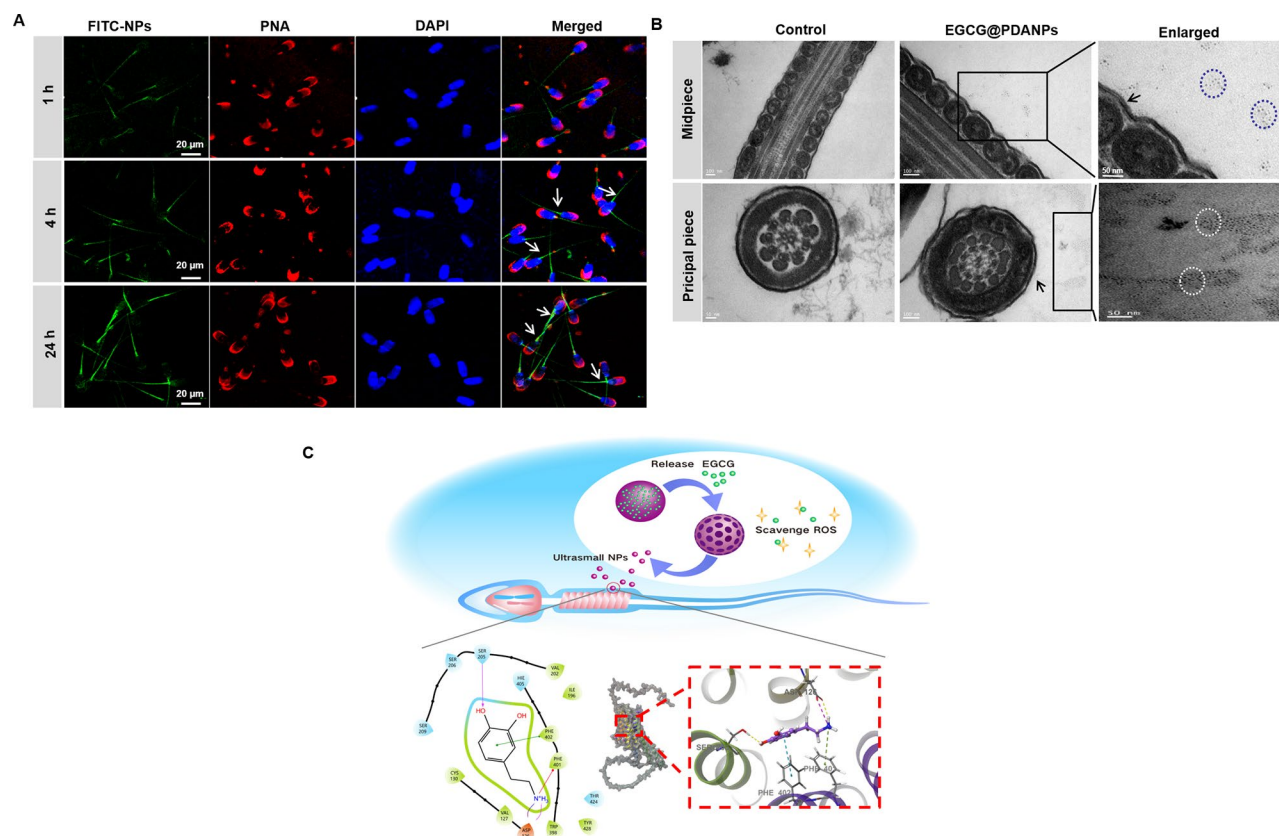


**Fig. 8** Interactions between EGCG@PDA NPs and sperm. **A.** localization of FITC-labeled EGCG@PDA NPs in sperm cells. **B.** TEM images of sperm interacted with EGCG@PDA NPs. **C.** 2D and 3D images of dopamine docking with D2DR receptors

free EGCG, PDA NPs, EGCG/PDA NPs mixture groups (Fig. 4), which might be attributed to the controlled-release of EGCG in the semen system and the synergistic effect of EGCG and PDA NPs, highlighting the superiority of nanotechnology in fabricating novel protectants.

Another primary finding of this study is that EGCG@PDA NPs could degrade into ultrasmall nanoparticles in response to ROS (Fig. 2) and these resulting ultrasmall nanoparticles could specifically target D2DR and activate the D2DR/cAMP/PKA signaling pathway to elevate protein phosphorylation levels in boar sperm (Figs. 6, 7 and 8). Previous studies have shown that nanoparticles with smaller diameters possess higher antioxidant capabilities [49], suggesting that this ROS-responsive character of EGCG@PDA NPs could be beneficial for pig semen preservation. Intriguingly, their diminutive size facilitates precise targeting of D2DR, further boosting the protective efficacy of EGCG@PDA NPs. Illustratively, D2DR is a crucial receptor primarily located into the midpiece of boar sperm, and it is involved in regulation of sperm function. For instance, D2DR stimulation increases tyrosine phosphorylation and accelerates boar sperm motility [27]. Additionally, dopamine also has been reported to enhance sperm motility characteristics and the acrosome response in humans, which are thought to be initiated

by tyrosine phosphorylation [28]. Mechanistically, since PDA nanoparticles were self-polymerized by free dopamine molecules, molecular docking in our study demonstrated that dopamine binds to the surface of the active pocket of D2DR via multiple hydrogen bonds and hydrophobic interactions (Fig. 8), further suggesting the role of D2DR in mediating the effect of our nano-protectant. Taken together, we speculated that the attachment of our nanoprotectant to sperm may trigger D2DR-mediated cAMP/PKA signaling, thereby enhancing p-PKAs and PTP levels.

Coincidentally, EGCG@PDA NPs-induced elevation in p-PKAs and PTP levels following a similar trend with that of sperm quality parameters, which was in accordance with the earlier reports on positive correlation between phosphorylation levels in sperm proteins and motility parameters [8]. This effect may be attributed to the fact that phosphorylation events can alter the activity, localization and interactions of proteins involved in sperm motility, thereby influencing their functionality. In brief, protein kinases, including PKA and protein tyrosine kinases, are involved in the phosphorylation of specific target proteins in sperm cells. Accordingly, these phosphorylation events occur on serine/threonine and tyrosine residues and subsequently modulate the activity

of molecular motors, ion channels, and cytoskeletal components, ultimately altering sperm motility [7, 56]. However, further research is needed to precisely identify the specific phosphorylated proteins in the cAMP/PKA signaling pathway and their specific functions in regulating sperm motility, which could aid in developing effective therapeutic strategies for prolonged semen preservation.

Comparatively, the EGCG@PDA NPs nano-protectant has its unique features and benefits, a comprehensive comparison with other nanoparticles reveals both strengths and limitations that require further improvement. Firstly, it shows excellent antioxidant properties, which can effectively protect sperm from oxidative damage during preservation, similar to the antioxidant nanoparticles such as cerium oxide nanoparticles [57], selenium nanoparticles [58], zinc oxide nanoparticles [59]. Additionally, EGCG@PDA NPs possess targeting ability to D2DR and hence activate D2DR/cAMP/PKA signaling pathway to regulate the protein phosphorylation status. This dual-task combination of oxidation resistance and up-regulation of protein phosphorylation confers EGCG@PDA NPs better protection efficiency compared with other nanoparticles with a single antioxidant function [60]. However, like other nanoparticles, there are still challenges such as limitations of the precise fate of EGCG@PDA NPs in boar semen. For instance, how long NPs are maintained in spermatozoa and whether NPs are continuously maintained in spermatozoa even during transit to the female reproductive tract, which need to be carefully addressed in future, clarifying these questions will help explain the protective effects of NPs on boar sperm storage as well as fertility.

## Conclusion

The durable and efficient antioxidant properties of EGCG@PDA NPs, their ability to disassemble into specific bio-targeting ultrasmall particles (<10 nm), and the up-regulation of protein phosphorylation levels via D2DR activated-cAMP/PKA signaling pathways rendered EGCG@PDA NPs as an elegant nano-protectant in semen systems for prolonging boar semen preservation. These findings provide valuable insights into the potential application of EGCG@PDA NPs as a novel strategy to enhance boar sperm quality and reproductive performance.

## Abbreviations

PDA NPs	Polydopamine nanoparticles
EGCG@PDA NPs	EGCG-loaded PDA NPs
D2DR	Phosphorylation of PKA substrates (P-PKAs) and protein tyrosine phosphorylation (PTP)
ROS	Reactive oxygen species
cAMP	Cyclic adenosine monophosphate PKA: protein kinase A
EGCG	Epigallocatechin gallate
DA	Dopamine
MDA	Malondialdehyde

SDS-PAGE	Sodium dodecyl sulfate polyacrylamide gel electrophoresis
T-AOC	Total antioxidant capacity
TEM	Transmission electron microscopy
DLS	Dynamic light scattering
FTIR	Fourier transform infrared spectroscopy
$\Delta\psi_m$	Mitochondrial membrane potential
MOT	Total motility
PRO	Progressive motility
PTKs	Protein tyrosine kinases
P-PKAs	Phosphorylation of PKA substrates
PTP	Protein tyrosine phosphorylation

## Supplementary Information

The online version contains supplementary material available at <https://doi.org/10.1186/s12951-025-03215-2>.

Supplementary Material 1

## Acknowledgements

Not applicable.

## Author contributions

WLR and LXH conceived this study and participated in experimental design. WLR, XMY and ZJ performed the experiment. LSS and MS analyzed completed the figures and data analysis. WLR wrote the manuscript draft. LXH, JSY and JYP checked and revised the manuscript. All authors read and approved the final manuscript.

## Funding

The authors gratefully acknowledge funding from Shanghai Agricultural Science and Technology Innovation Project (2023-02-08-00-12-F04601), National Nature Science Foundation of China (No. 32372876), and China Postdoctoral Science Foundation (No. 2021M702153 and No. 2022T150417).

## Data availability

No datasets were generated or analysed during the current study.

## Declarations

### Ethics approval and consent to participate

All animal experimental protocols were approved by the International Animal Care and Use Committee of Shanghai Jiao Tong University (No. IACUC-2020-035).

### Consent for publication

All authors approved the final manuscript and the submission to this journal.

### Competing interests

The authors declare no competing interests.

### Author details

<sup>1</sup>Shanghai Key Laboratory for Veterinary and Biotechnology, School of Agriculture and Biology, Shanghai Jiao Tong University, Shanghai 200240, China

<sup>2</sup>Department of Agriculture, Hetao College, Bayannur 015000, China

Received: 3 September 2024 / Accepted: 10 February 2025

Published online: 27 February 2025

## References

1. Pezo F, Romero F, Zambrano F, Sánchez RS. Preservation of boar semen: an update. *Repro Domest Anim.* 2019;54:423–34.
2. Xie Y, Chen Z, Wang Y, Peng X, Feng N, Wang X et al. Supplementation of schisandrin B in semen extender improves quality and oxidation resistance of boar spermatozoa stored at 4°C. *Anim (Basel).* 2023; 13.

3. Yang D, Yu X, Li X, Yu B, Peng H. Protective effects of L-cysteine and N-acetyl-L-cysteine on boar sperm quality during hypothermic liquid storage with bovine serum albumin as a protectant. *Theriogenology*. 2024;216:185–95.
4. Li X, Wang L, Liu H, Fu J, Zhen L, Li Y, et al. C(60) fullerenes suppress reactive oxygen species toxicity damage in boar sperm. *Nanomicro Lett*. 2019;11:104.
5. Sun L, Fan X, Zeng Y, Wang L, Zhu Z, Li R, et al. Resveratrol protects boar sperm in vitro via its antioxidant capacity. *Zygote*. 2020;28:417–24.
6. Fu J, Li Y, Wang L, Zhen L, Yang Q, Li P et al. Bovine serum albumin and skim-milk improve boar sperm motility by enhancing energy metabolism and protein modifications during liquid storage at 17°C. *Theriogenology*. 2017; 102.
7. Fu J, Yang Q, Li Y, Li P, Wang L, Li X. A mechanism by which Astragalus polysaccharide protects against ROS toxicity through inhibiting the protein dephosphorylation of boar sperm preserved at 4°C. *J Cell Physiol*. 2017; 233.
8. Li P, Yang Q, Li S, Sun H, Liu H, Li B et al. Candidates for reproductive biomarkers: protein phosphorylation and acetylation positively related to selected parameters of boar spermatozoa quality. *Anim Reprod Sci*. 2018; 197.
9. Visconti PE. Understanding the molecular basis of sperm capacitation through kinase design. *Proc Natl Acad Sci USA*. 2009;106:667–8.
10. Paul DR, Talukdar D, Ahmed FA, Lalrintluanga K, Kalita G, Tolenkhomba TC, et al. Effect of selenium nanoparticles on the quality and fertility of short-term preserved boar semen. *Front Vet Sci*. 2023;10:1333841.
11. Silvestre MA, Yáñez JL, Peña FJ, Santolaria P, Castelló-Ruiz M. Role of antioxidants in Cooled Liquid Storage of Mammal Spermatozoa. *Antioxid (Basel)*. 2021, 10.
12. Wang L, Zhang C, Hong Y, Li X, Li T, Gao A, et al. Integrating epigenetic modulators in nanofibers for synergistic gastric cancer therapy via epigenetic reprogramming. *Nano Lett*. 2021;21:298–307.
13. Zhang Y, Yang C, Wang W, Liu J, Liu Q, Huang F, et al. Co-delivery of doxorubicin and curcumin by pH-sensitive prodrug nanoparticle for combination therapy of cancer. *Sci Rep*. 2016;6:21225.
14. Yang J, Wang M, Zheng S, Huang R, Wen G, Zhou P, et al. Mesoporous polydopamine delivering 8-gingerol for the target and synergistic treatment to the spinal cord injury. *J Nanobiotechnol*. 2023;21:192.
15. Yin N, Zhang Z, Ge Y, Zhao Y, Gu Z, Yang Y, et al. Polydopamine-based nanomedicines for efficient antiviral and secondary injury protection therapy. *Sci Adv*. 2023;9:eadf4098.
16. Qiu J, Shi Y, Xia Y. Polydopamine nanobottles with Photothermal Capability for Controlled Release and related applications. *Adv Mater*. 2021;33:2104729.
17. Bao M, Wang K, Li J, Li Y, Zhu H, Lu M, et al. ROS scavenging and inflammation-directed polydopamine nanoparticles regulate gut immunity and flora therapy in inflammatory bowel disease. *Acta Biomater*. 2023;161:250–64.
18. Han J, Zheng S, Jin J, Wu T, Shi Y, Yang K, et al. Polydopamine-loaded prunetin nanomaterials activate DRD2 to reduce UV-induced inflammation by stabilizing and promoting Nrf2 nuclear translocation. *Acta Biomater*. 2023;169:556–65.
19. Xu H, Zhang Y, Zhang H, Zhang Y, Xu Q, Lu J, et al. Smart polydopamine-based nanoplatforams for biomedical applications: state-of-art and further perspectives. *Coordin Chem Rev*. 2023;488:215153.
20. Wang Z, Xu C, Lu Y, Wei G, Ye G, Sun T, et al. Microplasma electrochemistry controlled rapid preparation of fluorescent polydopamine nanoparticles and their application in uranium detection. *Chem Eng J*. 2018;344:480–6.
21. Yang X, Chen Y, Guo J, Li J, Zhang P, Yang H, et al. Polydopamine nanoparticles targeting ferroptosis mitigate intervertebral disc degeneration via reactive oxygen species depletion, iron ions chelation, and GPX4 ubiquitination suppression. *Adv Sci*. 2023;10:2207216.
22. Zhang X, Bai L, Zhou J, Gao H, Chen Q, Cui W, et al. Injectable microspheres adhering to the cartilage matrix promote rapid reconstruction of partial-thickness cartilage defects. *Acta Biomater*. 2024;179:220–33.
23. Zhu T, Wang H, Gu H, Ju L, Wu X, Pan W, et al. Melanin-like polydopamine nanoparticles mediating anti-inflammatory and rescuing synaptic loss for inflammatory depression therapy. *J Nanobiotechnol*. 2023;21:52.
24. Liu H, Qu X, Tan H, Song J, Lei M, Kim E, et al. Role of polydopamine's redox-activity on its pro-oxidant, radical-scavenging, and antimicrobial activities. *Acta Biomater*. 2019;88:181–96.
25. Zhang J, Zhou Y, Jiang Z, He C, Wang B, Wang Q, et al. Bioinspired polydopamine nanoparticles as efficient antioxidative and anti-inflammatory enhancers against UV-induced skin damage. *J Nanobiotechnol*. 2023;21:354.
26. Liang Z, He Y, Ieong CSU, Choi CHJ. Cell-nano interactions of polydopamine nanoparticles. *Curr Opin Biotech*. 2023;84:103013.
27. Ramírez AR, Castro MA, Angulo C, Ramió L, Rivera MM, Torres M, et al. The presence and function of dopamine type 2 receptors in boar sperm: a possible role for dopamine in viability, capacitation, and modulation of sperm motility. *Biol Reprod*. 2009;80:753–61.
28. Keyser S, van der Horst G, Maree L, Progesterone. Myo-Inositol, dopamine and prolactin present in follicular fluid have differential effects on sperm motility subpopulations. *Life (Basel)*. 2021; 11.
29. Kanno H, Kurata S, Hiradate Y, Hara K, Yoshida H, Tanemura K. High concentration of dopamine treatment may induce acceleration of human sperm motility. *Reprod Med Biol*. 2022;21:e12482.
30. Zhang Y, Lin H, Liu C, Huang J, Liu Z. A review for physiological activities of EGCG and the role in improving fertility in humans/mammals. *Biomed Pharmacother*. 2020;127:110186.
31. Gadani B, Bucci D, Spinaci M, Tamanini C, Galeati G. Resveratrol and epigallocatechin-3-gallate addition to thawed boar sperm improves in vitro fertilization. *Theriogenology*. 2017;90:88–93.
32. Wang L, Xiong M, Li S, Ma S, Jiang S, Wang H, et al. Beneficial effects of EGCG on boar sperm quality during liquid storage at 4°C are mediated by DRD2 receptor. *Theriogenology*. 2025;234:174–85.
33. Lin C, Cheng TM, Liu YC, Hsu FY, Shih CM, Tsai ML, et al. Dual-targeting EGCG/NO-supplying protein assembled nanoparticles with multi-synergistic effects against atherosclerosis. *Chem Eng J*. 2024;493:152755.
34. Cano A, Ettcheto M, Chang J-H, Barroso E, Espina M, Kühne BA, et al. Dual-drug loaded nanoparticles of Epigallocatechin-3-gallate (EGCG)/Ascorbic acid enhance therapeutic efficacy of EGCG in a APPsw/PS1dE9 Alzheimer's disease mice model. *J Control Release*. 2019;301:62–75.
35. Farabegoli F, Granja A, Magalhães J, Purgato S, Voltattorni M, Pinheiro M. Epigallocatechin-3-gallate delivered in nanoparticles increases cytotoxicity in three breast carcinoma cell lines. *ACS Omega*. 2022;7:41872–81.
36. Jiang P, Choi A, Swindle-Reilly KE. Controlled release of anti-VEGF by redox-responsive polydopamine nanoparticles. *Nanoscale*. 2020;12:17298–311.
37. Wang Y, Liu Y, Liu Y, Zhong J, Wang J, Sun L, et al. Remodeling liver microenvironment by L-arginine loaded hollow polydopamine nanoparticles for liver cirrhosis treatment. *Biomaterials*. 2023;295:122028.
38. Zhang M, Zhang F, Liu T, Shao P, Duan L, Yan J, et al. Polydopamine nanoparticles camouflaged by stem cell membranes for synergistic chemo-photothermal therapy of malignant bone tumors. *Int J Nanomed*. 2020;15:10183–97.
39. Ali Hassan H, Banchi P, Domain G, Vanderheyden L, Prochowska S, Nizański W. Mito-Tempo improves acrosome integrity of frozen-thawed epididymal spermatozoa in tomcats. *Front Vet Sci*. 2023; 10.
40. Skinner WM, Petersen NT, Unger B, Tang S, Tabarsi E, Lamm J, et al. Mitochondrial uncouplers impair human sperm motility without altering ATP content. *Biol Reprod*. 2023;109:192–203.
41. Pasciu V, Nieddu M, Sotgiu FD, Baralla E, Berlinguer F. An overview on assay methods to quantify ROS and enzymatic antioxidants in Erythrocytes and Spermatozoa of small domestic ruminants. *Animals*. 2023;13:2300.
42. Kuang M, Yu H, Qiao S, Huang T, Zhang J, Sun M, et al. A novel nano-antimicrobial polymer engineered with chitosan nanoparticles and bioactive peptides as promising food biopreservative effective against foodborne pathogen *E. coli* O157-caused epithelial barrier dysfunction and inflammatory responses. *Int J Mol Sci*. 2021;22:13580.
43. Yang Q, Wen Y, Wang L, Peng Z, Yeerken R, Zhen L, et al. Ca<sup>2+</sup> ionophore A23187 inhibits ATP generation reducing mouse sperm motility and PKA-dependent phosphorylation. *Tissue Cell*. 2020;66:101381.
44. Wang Y, Liu Q, Sun Q, Zheng L, Jin T, Cao H, et al. Exosomes from porcine serum as endogenous additive maintain function of boar sperm during liquid preservation at 17°C in vitro. *Theriogenology*. 2024;219:147–56.
45. Wang L, Li P, Wen Y, Yang Q, Zhen L, Fu J et al. Vitamin C exerts novel protective effects against cadmium toxicity in mouse spermatozoa by inducing the dephosphorylation of dihydroliipoamide dehydrogenase. *Reprod Toxicol*. 2017; 75.
46. Zhao W, Liu Z, Liang X, Wang S, Ding J, Li Z, et al. Preparation and characterization of epigallocatechin-3-gallate loaded melanin nanocomposite (EGCG@MNPs) for improved thermal stability, antioxidant and antibacterial activity. *LWT*. 2022;154:112599.
47. Yu X, Fan H, Wang L, Jin Z. Formation of polydopamine nanofibers with the aid of folic acid. *Angew Chem Int Ed*. 2014;53:12600–4.
48. Fan R, Chen C, Hou H, Chuan D, Mu M, Liu Z, et al. Tumor acidity and near-infrared light responsive dual drug delivery polydopamine-based nanoparticles for chemo-photothermal therapy. *Adv Funct Mater*. 2021;31:2009733.
49. Han J, Wang J, Shi H, Li Q, Zhang S, Wu H, et al. Ultra-small polydopamine nanomedicine-enabled antioxidation against senescence. *Mater Today Bio*. 2023;19:100544.

50. Xu M, Qi Y, Liu G, Song Y, Jiang X, Du B. Size-dependent in vivo transport of nanoparticles: implications for delivery, targeting, and clearance. *ACS Nano*. 2023;17:20825–49.
51. Augustine R, Hasan A, Primavera R, Wilson RJ, Thakor AS, Kevadiya BD. Cellular uptake and retention of nanoparticles: insights on particle properties and interaction with cellular components. *Mater Today Commun*. 2020;25:101692.
52. Li P, Yang Q, Li S, Sun H, Liu H, Li B, et al. Candidates for reproductive biomarkers: protein phosphorylation and acetylation positively related to selected parameters of boar spermatozoa quality. *Anim Reprod Sci*. 2018;197:67–80.
53. Hu B, Zhang H, Li Y, Xue Q, Yang M, Cao C, et al. Kojic acid inhibits pig sperm apoptosis and improves capacitated sperm state during liquid preservation at 17°C. *Mol Reprod Dev*. 2024;91:e23738.
54. Zhu Z, Kawai T, Umehara T, Hoque SAM, Zeng W, Shimada M. Negative effects of ROS generated during linear sperm motility on gene expression and ATP generation in boar sperm mitochondria. *Free Radical Bio Med*. 2019;141:159–71.
55. Zhu Z, Li W, Yang Q, Zhao H, Zhang W, Adetunji AO, et al. Pyrroloquinoline quinone improves ram sperm quality through its antioxidative ability during storage at 4°C. *Antioxidants*. 2024;13:104.
56. Li X, Wang L, Li Y, Fu J, Zhen L, Yang Q et al. Tyrosine phosphorylation of dihydrolipoamide dehydrogenase as a potential cadmium target and its inhibitory role in regulating mouse sperm motility. *Toxicology*. 2016; 357.
57. Hosseinmardi M, Siadat F, Sharafi M, Roodbari NH, Hezavehei M. Protective effect of cerium oxide nanoparticles on human sperm function during cryopreservation. *Biopreserv Biobank*. 2022;20:24–30.
58. Paul DR, Talukdar D, Ahmed FA, Lalrintluanga K, Kalita G, Tolenkhomba TC et al. Effect of selenium nanoparticles on the quality and fertility of short-term preserved boar semen. *Front Vet Sci*. 2024; 10.
59. Hozyen HF, Shamy AAE, Fattah EMAE, Sakr AM. Facile fabrication of zinc oxide nanoparticles for enhanced buffalo sperm parameters during cryopreservation. *J Trace Elem Min*. 2023;4:100058.
60. Asadi Z, Safari-Faramani R, Aghaz F. Effects of adding antioxidant nanoparticles on sperm parameters of non-human species after the freezing and thawing process: a systematic review and meta-analysis. *Anim Reprod Sci*. 2023;257:107323.

### Publisher's note

Springer Nature remains neutral with regard to jurisdictional claims in published maps and institutional affiliations.